Use of Hydrologic Landscape Classification to Diagnose Streamflow Predictability in Oregon

Patil, S.D.; Wigington, P.J.; Leibowitz, S.G.; Comeleo, R.L.

Journal of the American Water Resources Association

DOI:
10.1111/jawr.12143

Published: 18/11/2013

Peer reviewed version

Use of Hydrologic Landscape Classification to Diagnose Streamflow Predictability in Oregon

Sopan Patil, Parker J. Wigington, Jr., Scott G. Leibowitz, Randy L. Comeleo*

Submission to:

Journal of the American Water Resources Association

* Respectively, ORISE Postdoctoral Researcher (Patil), Research Hydrologist, retired (Wigington), Research Ecologist (Leibowitz), Ecologist (Comeleo), U.S. Environmental Protection Agency, National Health and Environmental Effects Research Laboratory, Western Ecology Division, 200 SW 35th St. Corvallis, Oregon (Email/Patil: sopan.patil@gmail.com).

Abstract

We implement a spatially lumped hydrologic model to predict daily streamflow at 88 catchments within Oregon, USA and analyze its performance using the Oregon Hydrologic Landscape (OHL) classification. OHL is used to identify the physio-climatic conditions that favor high (or low) streamflow predictability. High prediction catchments (Nash-Sutcliffe efficiency of $\sqrt{Q}$ (NS) > 0.75) are mainly classified as rain dominated with very wet climate, low aquifer permeability, and low to medium soil permeability. Most of them are located west of the Cascades Mountain Range. Conversely, most low prediction catchments (NS < 0.6) are classified as snow dominated with high aquifer permeability and medium to high soil permeability. They are mainly located in the volcano-influenced High Cascades region. Using a subset of 36 catchments, we further test if class-specific model parameters can be developed to predict at ungauged catchments. In most catchments, OHL class-specific parameters provide predictions that are on par with individually calibrated parameters (NS decline < 10%). However, large NS declines are observed in OHL classes where predictability is not high enough. Results suggest that higher uncertainty in rain-to-snow transition of precipitation phase and external gains/losses of deep groundwater are major factors for low prediction in Oregon. Moreover, regionalized estimation of model parameters is more useful in regions where conditions favor good streamflow predictability.

KEY TERMS: surface water hydrology, simulation, streamflow, watersheds, rivers/streams.

Introduction

Models in earth sciences, by definition, provide a simplified representation of real world processes and phenomena. For models in hydrology, the water balance concept is the fundamental principle through which various fluxes of water are connected and organized within a catchment [*Eagleson*, 1978; *Dooge*, 1986; *Kirkby*, 2006]. Through this organizing principle, a variety of hydrologic models have been developed over the years and successfully implemented at numerous catchments across the world [*Beven and Kirkby*, 1979; *Chiew and McMahon*, 1994; *Bergström*, 1995; *Edijatno et al.*, 1999; *Perrin et al.*, 2003]. However, research has also shown that there are limits to the physio-climatic conditions across which hydrologic models can provide good streamflow predictions [*Abdulla and Lettenmaier*, 1997; *Croke and Jakeman*, 2001; *Martinez and Gupta*, 2010; *Li et al.*, 2012]. Specifically, for the prediction of daily streamflow over long periods, studies have shown that catchments in certain regions (e.g., with arid climate, or with high groundwater influence) are typically more difficult to predict [*Ye et al.*, 1997; *Hay and McCabe*, 2002; *Biftu and Gan*, 2004; *Clark et al.*, 2008; *Fenicia et al.*, 2008; *Fenicia et al.*, 2011]. Unfortunately, a complete understanding of why hydrologic models perform remarkably well in some regions, and why they fail to do so in other regions, has still not been achieved.

The difficulty in predicting daily streamflow at a catchment potentially arises from three main sources: (1) there is uncertainty (or error) in the meteorological inputs, (2) some key hydrological processes unique to that catchment are either excluded or inappropriately represented in the hydrologic model structure, and/or (3) there are unknown (and perhaps unmeasurable) losses/gains of groundwater between the catchment and its surrounding region, which results in the violation of the water balance principle. The first source can be addressed by choosing meteorological forcing data of appropriate quality. A number of studies have shown that the quality of meteorological data used has a direct influence on the quality of modeled streamflow predictions [*Andréassian et al.*, 2001; *Bárdossy and Das*, 2008; *McMillan et al.*, 2011]. Recent studies such as *Vaze et al.* [2011] have further shown that better streamflow predictions are obtained with the use of a gridded meteorological dataset than with a single meteorological gage or a Theissen weighted average of multiple meteorological gages. The second source, hydrological process representation, can be addressed to some extent by using the top-down approach to hydrologic modeling [*Klemeš*, 1983; *Sivapalan et al.*, 2003]. In the top-down approach, a chosen model structure is first implemented at the catchment of interest and the model performance is compared with observed streamflow data. If the model performance is unsatisfactory, process components are either added to or removed from the model iteratively based on the available geophysical catchment data and/or the modeler's judgment on which processes are more important [*Jothityangkoon et al.*, 2001; *Farmer et al.*, 2003; *Tekleab et al.*, 2011]. While this approach has been shown to work at a few case-study catchments, the subjectivity involved in a modeler's decisions and the *ad hoc* nature of available geophysical data in different parts of the world makes this approach cumbersome and difficult to scale-up (i.e., apply consistently at a large number of catchments on a regional/continental scale). The third source, losses/gains of groundwater, is the most challenging to address due to our limited understanding of the conditions responsible for the exports or imports of water outside a catchment boundary. It is also difficult to quantify these losses and gains so that they can be explicitly accounted for in the water balance equations. While there have been studies using coupled surface – ground water models at catchment scales [*Sophocleous and Perkins*, 2000; *Maxwell and Miller*, 2005; *Ireson et al.*, 2006], the borehole water-table measurements required for the calibration of groundwater components are usually not available in the majority of catchments.

To overcome the restrictions in hydrologic characterization caused by limited data availability, scientists have long suggested the need to develop a hydrologically-based classification system for landscapes [*Woods*, 2002; *McDonnell and Woods*, 2004; *Wagener et al.*, 2007]. Such a classification system would ideally guide hydrologists in developing better conceptual models of catchment function [*McDonnell et al.*, 2007], and also narrow down the causes for potential pitfalls in predictability despite the lack of detailed site measurements. Although there have been numerous efforts over the years at developing a hydrologic classification system [*Mosley*, 1981; *Acreman and Sinclair*, 1986; *Wiltshire*, 1986; *Ogunkoya*, 1988; *Burn and Goel*, 2000], the study by *Wolock et al.* [2004] is perhaps the most comprehensive attempt at hydrologic classification over large scales (they covered the entire United States, including Alaska and Hawaii). This classification system was based on the Hydrologic Landscapes concept of *Winter* [2001], and conceptualized that landscape units with similar soil, climate, and terrain properties will have the same expected hydrologic behavior. Using this perceptual model, *Wolock et al.* [2004] classified the entire United States into 20 broad Hydrologic Landscape Regions (HLRs). Recently, *Wigington et al.* [2012] noted that, when viewed at the scale of an individual state within the US, inconsistencies can be found in the HLR classification system, primarily due to the coarse resolution of the data used by *Wolock et al.* [2004]. They suggested that a more detailed approach is required at the state level and proposed the Oregon Hydrologic Landscapes (OHL) classification, which uses a similar perceptual model as *Wolock et al.* [2004] but with higher resolution geophysical data than what are available at the national scale.

In this paper, our goal is to demonstrate that a hydrologically based landscape classification system can be effectively used to characterize the conditions at which a hydrologic model is more likely to perform well; and also to understand why it does not perform well in certain environments. Furthermore, a classification system may provide a readily available perceptual model of expected hydrologic behavior that can be compared against a mechanistic hydrologic model to detect inconsistencies. Classification may also play an important role in the characterization of hydrologic similarity among catchments and can help improve the predictability at ungauged catchments. Although a classification system typically assumes that similarity in physio-climatic properties translates into hydrologic similarity, a hydrologic model can verify whether catchments belonging to the same classification group truly have similar hydrologic behavior. As a specific example of this concept, we use a spatially lumped hydrologic model called EXP-HYDRO [*Patil and Stieglitz*, 2012] to simulate daily streamflow at 88 catchments within the state of Oregon, USA and compare its simulation performance against the OHL classification system of *Wigington et al.* [2012]. The mathematical structure of the EXP-HYDRO model forms our *a priori* hypothesis of a catchment's expected hydrologic behavior. The success or failure of this hypothesis (through good or bad prediction) at a catchment is then analyzed with respect to the OHL classification system. Specifically, we seek to (1) identify the physio-climatic properties that are more likely to be prevalent in high (and low) prediction catchments, and (2) test if a common regionalized set of model parameters is applicable to all the catchments that belong to the same classification unit. To our knowledge, there have been no previous studies that have analyzed the geographic patterns of streamflow predictions obtained through a hydrologic model within the context of a hydrologic classification framework. We would also like to note here that the concepts presented in this paper are generic in nature and can be readily implemented at different locations by using any other combination of hydrologic model and/or hydrologic classification system.

Data

We used the hydro-climatic data of 88 catchments located across the state of Oregon (see Figure 1). These catchments were selected from two different U.S. Geological Survey databases, viz., HCDN [*Slack et al.*, 1993] and GAGES [*Falcone et al.*, 2010], and are considered to be "reference" condition catchments (suggesting minimal anthropogenic impact on flow regime) in either of those databases. The drainage area of the catchments ranges from 8 km^2 to 1730 km^2, with a median drainage area of 265 km^2. The mean annual precipitation in the catchments ranges from 530 mm to 3300 mm, with a median value of 1700 mm. The Cascade Mountain Range traverses Oregon in the north – south direction, which creates a sharp contrast in climate among catchments to the east and west of the mountain range. The western catchments are characterized by a wet climate that is heavily influenced by the westerly winds of moisture-laden marine air from the Pacific Ocean. On the other hand, the eastern catchments are characterized by a drier climate (except at high elevations) mostly due to the rain-shadow effect created by the Cascade Mountains. Detailed descriptions of the climatic, geologic, and topographic variations within the state of Oregon can be found in *Wigington et al.* [2012].

The daily streamflow data was obtained from the USGS streamgages that are located at the outlet of all the 88 catchments. For the streamflow data, we considered the time-span ranging 60 years from water year 1951 to 2010. While every catchment did not have the data available for all those years, all catchments had continuous streamflow measurements for at least 15 years within this time-span. Daily precipitation and air temperature data were obtained from a gridded dataset of observed climate developed by *Maurer et al.* [2002]. This dataset is gridded at 1/8 degree (about 14 km) spatial resolution and covers the entire continental United States. For each catchment, the daily precipitation and air temperature time-series were obtained by taking an area-weighted average of the values from all the climate grids that are either fully or partially located within the catchment.

Methods

Hydrologic model

The Exponential Bucket Hydrologic Model (EXP-HYDRO; see Figure 2) is a spatially lumped hydrologic model [*Patil and Stieglitz*, 2012] that solves the following coupled water balance equations of the catchment and snow accumulation bucket stores at each time step:

$$\frac{dS}{dt} = P_r + M - ET - Q_{bucket} - Q_{spill} \quad (1a)$$

$$\frac{dS_s}{dt} = P_s - M \quad (1b)$$

where, S and S_s are the amounts of water stored in the catchment and snow accumulation buckets, respectively (unit: mm), P_s and P_r are the daily snowfall and rainfall amounts, respectively (unit: mm/day), ET is the actual evapotranspiration (unit: mm/day), Q_{bucket} is the runoff generated from the catchment bucket (unit: mm/day), Q_{spill} is the capacity-excess runoff that occurs when the catchment bucket is full (unit: mm/day), and M is the snowmelt (unit: mm/day). The incoming daily precipitation is classified as snowfall or rainfall based on the following condition:

If $T_a < T_{\min}$,

$$\begin{aligned} P_s &= P \\ P_r &= 0 \end{aligned} \quad (2a)$$

Else,

$$\begin{aligned} P_s &= 0 \\ P_r &= P \end{aligned} \tag{2b}$$

where, T_a is actual daily air temperature (unit: °C) and $T_{\min}$ is the air temperature (unit: °C) below which any precipitation in the catchment falls as snow (into the snow accumulation bucket). Snowmelt M from the snow accumulation bucket is modeled using a thermal degree-day model as follows:

If $T_a > T_{\max}$,

$$M = \min\{S_s, D_f \cdot (T_a - T_{\max})\} \tag{3a}$$

Else,

$$M = 0 \tag{3b}$$

where, D_f is the thermal degree-day factor (unit: mm/day/°C), and $T_{\max}$ is the air temperature (unit: °C) above which accumulated snow in the snow accumulation bucket begins to melt. Evapotranspiration ET is calculated as a fraction of the potential evapotranspiration (PET), and depends on the amount of actual stored water (S) in the catchment bucket relative to the bucket's storage capacity ($S_{\max}$):

$$ET = PET \cdot \left(\frac{S}{S_{\max}} \right) \tag{4}$$

PET (unit: mm/day) is calculated from the daily air temperature data using Hamon's formulation [*Hamon*, 1963]. The runoff generated from the catchment bucket depends on the amount of water stored in it and is calculated using a TOPMODEL [*Beven and Kirkby*, 1979] type equation:

If $S \le S_{\max}$,

$$\begin{aligned} Q_{bucket} &= Q_{\max} \cdot \exp(-f \cdot (S_{\max} - S)) \\ Q_{spill} &= 0 \end{aligned} \quad (5a)$$

If $S > S_{\max}$,

$$\begin{aligned} Q_{bucket} &= Q_{\max} \\ Q_{spill} &= S - S_{\max} \end{aligned} \quad (5b)$$

where, $Q_{\max}$ is the runoff produced (unit: mm/day) when the bucket storage reaches its maximum capacity, and f is the parameter controlling the storage-dependent exponential decline in bucket generated runoff (unit: 1/mm). It must be noted that although alternative forms of Equation 5a have been proposed by some studies (e.g., linear, parabolic), the exponential version shown here is the most widely used variant of the TOPMODEL equation [*Ambroise et al.*, 1996; *Li et al.*, 2011]. Daily streamflow at the catchment outlet is the sum of Q_{bucket} and Q_{spill}. The coupled ordinary differential equations (Equation 1a and 1b) are solved simultaneously at each time step using the 4th order Runge-Kutta numerical scheme.

Calibration of model parameters

The EXP-HYDRO model consists of six free calibration parameters: f, $Q_{\max}$, $S_{\max}$, D_f, $T_{\min}$, and $T_{\max}$. For each catchment, we calibrated these parameters with 50,000 Monte Carlo simulations [*Vaché and McDonnell*, 2006; *Patil and Stieglitz*, 2012]. Table 1 shows the parameter ranges used for generating the 50,000 uniformly distributed random samples of the six parameters. Observed daily streamflow data from the first available 10 years for the catchment was chosen for model optimization (calibration period), whereas the consecutive 5 years (years 11 to 15) were chosen as the validation period. We used Nash Sutcliffe efficiency [*Nash and Sutcliffe*, 1970] of square root values of daily streamflow as the objective function:

$$NS = 1 - \frac{\sum_{i=1}^{n}(\sqrt{Q_{obs,i}} - \sqrt{Q_{pred,i}})^2}{\sum_{i=1}^{n}(\sqrt{Q_{obs,i}} - \sqrt{\overline{Q}_{obs}})^2} \qquad (6)$$

where, $Q_{pred,i}$ and $Q_{obs,i}$ are the predicted and the observed streamflow values on the i^{th} day respectively, $\overline{Q}_{obs}$ is the mean of all the observed streamflow values and n is the total number of days in the time series. Nash Sutcliffe efficiency is the most widely used metric for calibration and evaluation of hydrologic models that provide continuous simulation over a long period [*Legates and McCabe*, 1999; *Krause et al.*, 2005]. There are three commonly used variants of the Nash Sutcliffe efficiency formula: untransformed (Q), square root transformed ($\sqrt{Q}$), and log transformed ($\log Q$) [*Oudin et al.*, 2006]. As an objective function, NS (Q) has a tendency to over-emphasize the matching of high flow values at the expense of low flows, whereas NS ($\log Q$) tends to do the opposite. NS ($\sqrt{Q}$) is a balance between these two extremes and focuses on matching the overall hydrograph, albeit at the expense of very high and very low flow values. Since our objective in this study was to match the overall hydrologic dynamics of a catchment, we used NS ($\sqrt{Q}$) as the objective function (Equation 6, and referred to simply as NS henceforth). The value of NS ranges from negative infinity to 1, with NS = 1 being a perfect fit between the model and observed data. Out of the 50,000 parameter sets used for calibration at each catchment, we selected a single parameter set that provided the maximum value of NS as the optimal parameter set. While the uncertainty in parameter values due to equifinality (i.e., multiple combinations of parameter values providing similar model performance) exists in most hydrologic models [*Beven and Freer*, 2001], we have restricted our focus to characterizing the best performance that is achievable with the EXP-HYDRO model at each catchment.

Oregon Hydrologic Landscapes (OHL) classification at catchment scale

Wigington et al. [2012] have used a hydrologic landscape unit (HLU; referred to as assessment unit in their paper) as the fundamental area to which a classification code is assigned based on its physio-climatic properties. Every HLU is either a first-order or an incremental sub-catchment that consists of a stream reach and a contributing hillslope. The HLUs were delineated within Oregon by using the following procedure: (1) extract the stream network from USGS National Elevation Dataset's 30 m DEM using a 25 km^2 minimum drainage area threshold for channel initiation, and (2) divide the landscape into HLUs along the stream nodes. *Wigington et al.* [2012] divided the state of Oregon into 5660 HLUs and classified the HLUs (using available climatic and geophysical data) based on five categories: annual climate, seasonality of water surplus, aquifer permeability, terrain, and soil permeability. The different classification codes within each category are summarized in Table 2. Based on these codes, an individual HLU is assigned a multi-letter OHL class. For instance, a HLU that is assigned an OHL class "VwLML" has the following physio-climatic properties: very wet climate, winter seasonality of water surplus, low aquifer permeability, mountainous terrain, and low soil permeability. The underlying assumption is that the HLUs that have the same OHL class are expected to have similar hydrologic behavior. Detailed information about the procedure for obtaining HLUs within Oregon and development of the OHL classes can be found in *Wigington et al.* [2012].

A catchment typically consists of an aggregation of multiple HLUs (see Figure 3). However, some small catchments can contain only a single first-order HLU. In fact, 37 out of the 88 catchments in this study contain only one HLU. For the 51 catchments that contain multiple HLUs, we defined their OHL catchment class by first considering each of the five physio-climatic categories separately and then identifying the class within each category that covers the largest area within the catchment (see Supplementary Table). For the 37 catchments containing only one HLU, the class associated with that HLU was assigned as the OHL catchment class. Detailed information about the OHL classes for all 88 catchments is provided in the Supplementary Table.

Results

Figure 4a shows the box-and-whisker plot of NS values of all the 88 catchments for the calibration and validation periods. The median NS values for calibration and validation period were 0.78 and 0.75 respectively. NS values of catchments for the validation period varied across a slightly larger range than those for the calibration period. Figure 4b shows the 1:1 relationship of NS values for the calibration and validation periods. Although the difference in model performance between those two periods is low in most catchments, large deviations can be found in a few catchments with low NS values.

Based on the NS value of streamflow calibration, we divided the 88 Oregon catchments into three hydrologic predictability groups: Group 1 (high predictability; $NS > 0.75$), Group 2 (medium predictability; $0.75 \geq NS \geq 0.6$), and Group 3 (low predictability; $0.6 > NS$). We followed *Martinez and Gupta* [2010] to set $NS > 0.75$ as a condition for high predictability catchments and *Patil and Stieglitz* [2012] to set $NS < 0.6$ as a condition for low predictability catchments. The remaining catchments ($0.75 \geq NS \geq 0.6$) were then assigned into the medium predictability group. Figure 5 shows the geographic distribution of catchments classified into the three predictability groups. The Group 1 catchments (49 in total, ~ 56%) are predominantly located in the westernmost part of the state. Most are along the Oregon Coast Range, followed by some catchments on the western side of the Cascade Mountains (Western Cascades), and only three catchments are in the eastern part of the state (east of the Cascade Mountains). The Group 2 catchments (14 in total, ~

16%) are mostly on the western side of the Cascade Mountains, but many of them are located closer to the mountain range than the Group 1 catchments. Five Group 2 catchments are located on the eastern side of the Cascade Mountains. The majority of Group 3 catchments (25 in total, ~ 28%) are located on either side of, but in the close vicinity to, the Cascade Mountains. Almost all the catchments that are nearest to the eastern side of the Cascade Mountains belong to Group 3. These catchments contain the tributaries of the Deschutes River. A few Group 3 catchments are also located in the eastern and northeastern parts of Oregon.

We next analyzed how the three hydrologic predictability groups relate to the OHL classification at the catchment scale. Each of the five physio-climatic categories (annual climate, seasonality, aquifer permeability, terrain, and soil permeability) were considered separately, and we calculated the extent to which each class is represented in the high, medium, and low predictability catchments (Groups 1 – 3). Table 3 summarizes the presence of each physio-climatic class within Group 1 – 3 catchments. Below, we provide a brief description of the major trends in each category.

For annual climate, the majority of catchments in all three predictability groups have either a wet (W) or a very wet (V) climate. This is not surprising since the geographic distribution of the 88 catchments is heavily skewed towards the wetter western part of Oregon. Nonetheless, the proportion of V climate class gradually decreases from Group 1 to Group 3 catchments, whereas the proportions of drier climate classes (M and D) show the opposite trend. For the seasonality of water surplus, a clear contrast is observed among the different predictability groups. As we move from Group 1 to Group 3, the extent of winter (w) seasonality class decreases rapidly from 92% in Group 1 to 28% in Group 3. On the other hand, spring (s) seasonality class is present in only 8% of the Group 1 catchments, but present in 68% of the Group 3 catchments. Only one catchment has a summer (u) seasonality class, and it belongs to Group 3. The aquifer permeability category also shows a sharp contrast between Group 1 and Group 3 catchments. Low (L) aquifer permeability is dominant among the Group 1 catchments (84%), whereas high (H) aquifer permeability is dominant among the Group 3 catchments (56%). The Group 2 catchments are dominated by the H aquifer permeability class (50%), followed by L (29%) and M (21%) classes. The terrain category is not useful as an explanatory variable in this exercise because all 88 catchments have the mountain (M) terrain class. For soil permeability, the majority of catchments in all three groups have either low (L) or medium (M) soil permeability. However, catchments with high (H) soil permeability are exclusive to Group 3.

The OHL classification hypothesizes that landscape units (or catchments) having the same OHL class should have similar hydrologic behavior. We tested this hypothesis using the following procedure: (1) group all the catchments that have the same OHL class; (2) using the grouped catchments from step 1, calculate the average value of all six parameters of the EXP-HYDRO model; (3) simulate the daily streamflow of all catchments within the group using average parameters from step 2, and calculate the decline in NS value compared to that from individual catchment calibration case. Only four OHL classes were available to test this procedure, since other classes did not have sufficient number of catchments. These four classes are: VwLML (9 catchments), VwLMM (12 catchments), WwLML (6 catchments), and WwLMM (9 catchments). Table 4 shows the range of optimal values of the EXP-HYDRO model parameters for catchments among the four OHL classes, and also their coefficient of variation (CV) within each class. Out of the 6 model parameters, f consistently has the smallest value of CV in all four classes. This indicates that the optimal value of f varies the least for catchments within an individual OHL class. Interestingly, the study by *Patil and Stieglitz* [2012] has shown that f is also the most sensitive (and identifiable) parameter of the EXP-HYDRO model. Table 5 shows the decline in model performance when using class averaged parameters compared to the individually calibrated parameters. The average decline in model performance was the lowest for the VwLML class (1%) and the highest for the WwLMM class (13%). Figure 6 shows the relationship between the NS value of a catchment using calibrated parameter set and the % decline in NS when the class-assigned common parameter set is used (for the 36 catchments in four OHL classes). Catchments with a high calibrated NS show the least performance decline, and the % decline in NS has an increasing trend with decreasing calibrated NS values. Of the 36 catchments considered in this analysis, only 5 catchments showed a decline in model performance of greater than 10%. Remarkably, none of the 9 catchments in the VwLML class showed a model performance decline above 4%.

Discussion

Results show that distinct patterns of streamflow predictability are obtained by implementing the EXP-HYDRO model within the state of Oregon (Figure 5). While studies have shown that wet climate tends to be favorable for obtaining good model predictions at a catchment [*Abdulla and Lettenmaier*, 1997; *Parajka et al.*, 2005; *Martinez and Gupta*, 2010], our results suggest that climate alone is insufficient to determine whether high or low predictability can be expected at a certain place. About 72% of the Group 3 catchments (low predictability; NS < 0.6) are classified as having either a wet (W) or very wet (V) climate. Based on the dominant classification within each of the OHL category (Table 3), we expect that a catchment in Oregon belonging to either the VwLMM or VwLML class has the greatest likelihood of being a high predictability catchment. In other words, a very wet climate, winter seasonality of water surplus, low aquifer permeability, mountainous terrain, and low to medium soil permeability is the most favorable combination of physio-climatic properties for obtaining high simulation performance with the EXP-HYDRO model. Conversely, the low prediction catchments in Oregon show a propensity towards spring seasonality of water surplus, high aquifer permeability, and medium to high soil permeability (see Table 3).

An important advantage of using the OHL classification system is that it reveals multiple physio-climatic factors that can affect streamflow predictions and therefore provides clues into the reasons for poor model behavior at a catchment. For instance, 14 out of the 25 Group 3 catchments and 7 out of the 14 Group 2 catchments are classified as having high aquifer permeability. High aquifer permeability in a catchment suggests a greater likelihood of having losses/gains with external groundwater sources that are difficult to quantify. The majority of Group 2 and 3 catchments with high aquifer permeability are located in or near the region closest to the Cascade Mountains (see Figure 5), which is commonly referred to as the High Cascades. The geology of this region is heavily influenced by relatively recent volcanic eruptions and lava flows, which have created complex patterns of groundwater flow [*O'Connor and Grant*, 2003; *Jefferson et al.*, 2006; *Tague et al.*, 2008]. This is in sharp contrast with the Western Cascades region which is located to the west of the High Cascades and consists of older, more weathered, and impermeable volcanic bedrock [*Mayer and Naman*, 2011]. *Tague and Grant* [2004] compared the streamflow regimes of catchments in the Western and High Cascades and showed that the above mentioned differences in geology have a direct impact on hydrologic response within each region. Specifically, rivers in the Western Cascades are runoff-dominated with fast recession rates and low summer baseflow, whereas rivers in the High Cascades are groundwater-dominated with more uniform flows, slower recession rates, and higher summer baseflow [*Safeeq et al.*, 2013]. *Wigington et al.* [2012]

illustrated the Metolius River as an example of a High Cascades catchment whose flow regime is significantly influenced by external groundwater interaction. Therefore, streamflow modeling in an environment such as the High Cascades is most likely to require an explicit representation of the external groundwater gains/losses, but at the cost of additional input data that might not be readily available in most places. The EXP-HYDRO model used in this paper does not explicitly account for groundwater gains/losses outside of the catchment boundary. *Manga* [1997] implemented an unconfined aquifer flow model, based on Boussinesq's equation for unsteady subsurface flow, at four spring-dominated tributaries of the Deschutes River near the High Cascades. Although the model provided good streamflow predictions, *Manga* [1997] used streamflow measurements from a nearby runoff-dominated catchment as a proxy for external recharge into the unconfined aquifer model. In the absence of a nearby "proxy" catchment, estimation of aquifer recharge in such a model is likely to induce high uncertainty and reduce the confidence in model predictions. *Gannett and Lite* [2004] coupled a groundwater flow model (MODFLOW) with a streamflow routing model to simulate discharge at the Upper Deschutes Basin. However, they used water-level measurements from 983 wells to calibrate the coupled model. The availability of such data cannot always be guaranteed at a catchment.

Spring seasonality of water surplus is another dominant feature among the lower predictability (Group 2 and 3) catchments. Spring seasonality indicates that the hydrologic regime of a catchment is noticeably influenced by spring snowmelt [*Wigington et al.*, 2012]. Our dataset contains 28 catchments with spring seasonality, of which 24 (86%) belonged to Group 2 and 3. However, out of these 24 catchments, 15 catchments (63%) have high aquifer permeability as a dominant feature. This suggests that isolating the individual impact of either high aquifer permeability or spring snowmelt on poor model prediction is not so straightforward for many catchments in Oregon. Figure 7 shows the relationship of NS with the inter-annual coefficient of variation (CV) of precipitation (P) and air temperature (T) (calculated from the 15 years used for calibration and validation) of all our study catchments with NS > 0. No significant trend exists in the relationship between NS and the CV of P (r^2 = 0.02, p value = 0.22), which suggests that a year-to-year change in the amount of precipitation does not have much effect on streamflow predictability. On the other hand, a statistically significant trend exists in the relationship between NS and the CV of T (r^2 = 0.47, p value < 0.01), such that the inter-annual variability in air temperature increases with decrease in NS. This has important ramifications for the catchments that are located in the rain/snow transition zones near the High Cascades, since small changes in air temperature can have a significant impact on the amount of snow accumulation at a catchment in a given year. Our results suggest that high year-to-year variability in air temperature increases the uncertainty in the phase of precipitation (i.e., how much snow a catchment typically expects), and is detrimental to streamflow predictability. Although the EXP-HYDRO model uses a simple thermal degree-day model to represent the snow processes, it is not clear whether a more complex snow model, that explicitly simulates the altitude effects [*Blöschl et al.*, 1991; *Corbari et al.*, 2009], sublimation [*MacDonald et al.*, 2010], variable lapse rates [*Nolin and Daly*, 2006], and/or ground temperature [*Stieglitz et al.*, 2001], can lead to any improvements in the streamflow prediction skills. It is important to note that such an increase in the complexity of a snow model usually requires additional input data, which might not be available in many places.

Prediction of streamflow at ungauged catchments is an important factor that has long motivated hydrologists towards the development of classification systems [*Mosley*, 1981; *McDonnell and Woods*, 2004; *Wagener et al.*, 2007]. In this study, we tested whether a class-assigned common parameter set of the EXP-HYDRO model can provide simulation performance that is close enough to the performance obtained with individually calibrated parameters. While this analysis was limited to only four OHL classes, our results showed that implementation of a common parameter set for an entire OHL class provides near optimal (less than 10% deterioration) performance in most catchments (31 out of 36; see Table 5). This suggests that, for the most part, catchments within the same class tend to have similar hydrologic behavior, thereby providing an independent validation of the OHL classification system. Parameter transfer based on physical catchment similarity has generally yielded mixed results in the past, where some studies have shown good performance at ungauged catchments [*Parajka et al.*, 2005; *Young*, 2006], while others have suggested that in certain cases, a mismatch exists between physical and hydrologic similarity [*Kokkonen et al.*, 2003; *Oudin et al.*, 2010]. Of the four OHL classes, the WwLMM class contains the most catchments with a high decline in NS (3 out of 9 catchments in that class have > 10% NS decline). Interestingly, the average calibrated NS value of catchments is also the lowest in the WwLMM class (avg. NS = 0.75). In comparison, the other three classes have higher average calibrated NS (VwLML = 0.90; VwLMM = 0.84; WwLML = 0.81). These findings are suggestive of an inherent link between similarity among catchments, in terms of model parameters and hydrologic landscape characteristics, and the hydrologic predictability of that catchment group/type. If catchments within a particular class are highly predictable (e.g., VwLML), their model parameters are more likely to be similar and therefore easily transferrable to an ungauged catchment within the same class (see Table 4). On the other hand, physio-climatic similarity among catchments (as characterized by OHL) is less useful if the model performance for that class of catchments is not high enough to begin with, perhaps due to some hydrologic characteristics (such as groundwater influence) that are difficult to incorporate into a regional classification scheme.

Caveats

We made several assumptions in our choice of the catchment data, classification scheme, and the hydrologic model that can potentially influence the findings of this study. While Oregon covers a large and diverse geographic area of the Pacific Northwest, the 88 catchments in this study were not evenly distributed throughout the state, with the majority of them located in the western part. This skew in the geographic distribution increased the number of catchments having OHL classes that are more prevalent in western Oregon and decreased the number of catchments having classes that are more typical of eastern Oregon, such as drier climate and spring or summer seasonality. Another limitation was the lack of diversity in the OHL classes within our data. Theoretically, there are 486 possible classes in the OHL classification system. Of these, 157 classes can be found in Oregon at the HLU level [*Wigington et al.*, 2012]. However, at the aggregated catchment level, only 19 unique OHL classes were manifested among the 88 catchments in this study (see Supplementary Table). Furthermore, the four most common OHL classes (VwLML, VwLMM, WwLML, and WwLMM) that we considered for the analysis of ungauged catchments were quite similar to each other, and prevented us from taking full advantage of the high hydrologic diversity that exists within Oregon. The choice of hydrologic classification scheme also had a major influence on our geographic interpretations of model predictability. For instance, *Wigington et al.* [2012] used five types of physio-climatic data that they considered to be relevant for hydrologic classification, and then made further subjective decisions on how many classes can exist within each data type. Modifications in either of those decisions will change the spatial distribution of landscape classes. The method that we used for aggregating the OHL classes of individual HLUs to the catchment scale could also affect our results. We selected the landscape class in each of the five categories that had maximum areal coverage within the catchment.

However, this method is less likely to be effective if there is high internal heterogeneity in the physio-climatic properties of the catchment. Lastly, the choice of input data and model structure play an important role on the observed spatial patterns of model predictions. While we used high quality gridded meteorological data [*Maurer et al.*, 2002] as model inputs, estimates of rain and snow tend to be poorer at high elevations. In terms of the model structure, we used a single bucket spatially lumped model that has been tested over a large number of catchments within the continental US [*Patil and Stieglitz*, 2012] and represents the hydrological processes that are prevalent in most catchments. While the EXP-HYDRO model was used as a specific example for the diagnosis of model behavior, the methods described in the paper can be readily used to analyze the strengths and weaknesses of different types of hydrologic models.

Concluding Remarks

This study focused on testing whether a hydrologically based landscape classification system can improve our understanding of why a hydrologic model performs remarkably well in some regions, and why it fails to do so in other regions. Using the EXP-HYDRO model and OHL classification as examples, we simulated daily streamflow in 88 catchments within Oregon, USA and compared the model predictability with the OHL classes of the catchments. We further tested whether class-specific model parameters can be developed and successfully implemented at ungauged catchments with similar OHL class. The main contribution of this paper is in showing that a hydrologic classification system is an efficient tool for analyzing a hydrologic model's strengths and weaknesses across a large number of catchments, thereby making it easier to identify and understand where the model weaknesses come from. Our results demonstrated that a hydrologically-based landscape classification system like OHL [*Wigington et al.*, 2012] can be effectively used to identify conditions that favor good streamflow predictability with a hydrologic model like EXP-HYDRO and also to constrain the potential causes for poor predictability at a catchment. This improved understanding of model success/failure can guide hydrologists during the revision of model structures using a top-down approach. Within the state of Oregon, a very wet climate, winter seasonality of water surplus, low aquifer permeability, mountainous terrain, and low to medium soil permeability is the most favorable combination of physio-climatic properties for high simulation performance with the EXP-HYDRO model. Results also showed that the OHL class-specific common parameters provide model performance that is almost on par with individually calibrated parameters in most catchments. However, performance deterioration with the class-specific common parameters is likely to be greater if the predictability of that OHL class is not high to begin with. This has important ramifications for estimating model parameters at ungauged catchments. Specifically, regionalized estimation of model parameters is more likely to be more useful in regions that have physio-climatic conditions that favor good hydrologic predictability.

Supporting Information

Additional supporting information may be found in the online version of this article:

Supplementary Table S1: OHL class obtained for all 88 Oregon catchments.

Acknowledgments

We are thankful to C. Rhett Jackson, Bob Ozretich, and three anonymous reviewers for valuable comments and suggestions that have greatly improved this paper. The first author was supported by ORISE postdoctoral fellowship for the duration of this study. The information in this document has been funded entirely by the U.S. Environmental Protection Agency. This manuscript has been subjected to Agency review and has been approved for publication. Mention of trade names or commercial products does not constitute endorsement or recommendation for use.

Literature Cited

Abdulla, F. A., and D. P. Lettenmaier (1997), Development of regional parameter estimation equations for a macroscale hydrologic model, *Journal of Hydrology*, *197*(1-4), 230-257, doi: 10.1016/s0022-1694(96)03262-3.

Acreman, M. C., and C. D. Sinclair (1986), Classification of drainage basins according to their physical characteristics; an application for flood frequency analysis in Scotland, *Journal of Hydrology*, *84*(3-4), 365-380, doi: 10.1016/0022-1694(86)90134-4.

Ambroise, B., K. Beven, and J. Freer (1996), Toward a Generalization of the TOPMODEL Concepts: Topographic Indices of Hydrological Similarity, *Water Resources Research*, *32*(7), 2135-2145, doi: 10.1029/95wr03716.

Andréassian, V., C. Perrin, C. Michel, I. Usart-Sanchez, and J. Lavabre (2001), Impact of imperfect rainfall knowledge on the efficiency and the parameters of watershed models, *Journal of Hydrology*, *250*(1–4), 206-223, doi: http://dx.doi.org/10.1016/S0022-1694(01)00437-1.

Bárdossy, A., and T. Das (2008), Influence of rainfall observation network on model calibration and application, *Hydrology and Earth System Sciences*, *12*(1), 77-89, doi: 10.5194/hess-12-77-2008.

Bergström, S. (1995), The HBV model, in *Computer models of watershed hydrology*, edited by V. P. Singh, pp. 443–476, Water Resources Publications, Colorado.

Beven, K. J., and M. J. Kirkby (1979), A physically based, variable contributing area model of basin hydrology / Un modèle à base physique de zone d'appel variable de l'hydrologie du bassin versant, *Hydrological Sciences Bulletin*, *24*(1), 43-69, doi: 10.1080/02626667909491834.

Beven, K. J., and J. Freer (2001), Equifinality, data assimilation, and uncertainty estimation in mechanistic modelling of complex environmental systems using the GLUE methodology, *Journal of Hydrology*, *249*(1-4), 11-29, doi: 10.1016/s0022-1694(01)00421-8.

Biftu, G. F., and T. Y. Gan (2004), A semi-distributed, physics-based hydrologic model using remotely sensed and Digital Terrain Elevation Data for semi-arid catchments, *International Journal of Remote Sensing*, *25*(20), 4351-4379, doi: 10.1080/01431160310001654374.

Blöschl, G., R. Kirnbauer, and D. Gutknecht (1991), Distributed Snowmelt Simulations in an Alpine Catchment: 1. Model Evaluation on the Basis of Snow Cover Patterns, *Water Resources Research*, *27*(12), 3171-3179, doi: 10.1029/91wr02250.

Burn, D. H., and N. K. Goel (2000), The formation of groups for regional flood frequency analysis, *Hydrological Sciences Journal*, *45*(1), 97-112, doi: 10.1080/02626660009492308.

Chiew, F., and T. McMahon (1994), Application of the daily rainfall-runoff model MODHYDROLOG to 28 Australian catchments, *Journal of Hydrology*, *153*(1-4), 383-416, doi: 10.1016/0022-1694(94)90200-3.

Clark, M. P., A. G. Slater, D. E. Rupp, R. A. Woods, J. A. Vrugt, H. V. Gupta, T. Wagener, and L. E. Hay (2008), Framework for Understanding Structural Errors (FUSE): A modular framework to diagnose differences between hydrological models, *Water Resources Research*, *44*, W00B02, doi: 10.1029/2007wr006735.

Corbari, C., G. Ravazzani, J. Martinelli, and M. Mancini (2009), Elevation based correction of snow coverage retrieved from satellite images to improve model calibration, *Hydrology and Earth System Sciences*, *13*(5), 639-649, doi: 10.5194/hess-13-639-2009.

Croke, B. F. W., and A. J. Jakeman (2001), Predictions in catchment hydrology: an Australian perspective, *Marine and Freshwater Research*, *52*(1), 65-79, doi: 10.1071/MF00045.

Dooge, J. C. I. (1986), Looking for hydrologic laws, *Water Resources Research*, *22*(9S), 46S-58S, doi: 10.1029/WR022i09Sp0046S.

Eagleson, P. S. (1978), Climate, soil, and vegetation: 1. Introduction to water balance dynamics, *Water Resources Research*, *14*(5), 705-712, doi: 10.1029/WR014i005p00705.

Edijatno, N. De Oliveira Nascimento, X. Yang, Z. Makhlouf, and C. Michel (1999), GR3J: a daily watershed model with three free parameters, *Hydrological Sciences Journal*, *44*(2), 263-277, doi: 10.1080/02626669909492221.

Falcone, J. A., D. M. Carlisle, D. M. Wolock, and M. R. Meador (2010), GAGES: A stream gage database for evaluating natural and altered flow conditions in the conterminous United States, *Ecology*, *91*(2), 621-621, doi: 10.1890/09-0889.1.

Farmer, D., M. Sivapalan, and C. Jothityangkoon (2003), Climate, soil, and vegetation controls upon the variability of water balance in temperate and semiarid landscapes: Downward approach to water balance analysis, *Water Resources Research*, *39*(2), 1035, doi: 10.1029/2001wr000328.

Fenicia, F., D. Kavetski, and H. H. G. Savenije (2011), Elements of a flexible approach for conceptual hydrological modeling: 1. Motivation and theoretical development, *Water Resources Research*, *47*(11), W11510, doi: 10.1029/2010wr010174.

Fenicia, F., H. H. G. Savenije, P. Matgen, and L. Pfister (2008), Understanding catchment behavior through stepwise model concept improvement, *Water Resources Research*, *44*(1), W01402, doi: 10.1029/2006wr005563.

Gannett, M. W., and K. E. Lite (2004), Simulation of regional ground-water flow in the upper Deschutes Basin, Oregon, *Water-Resources Investigations Report 03-4195*, US Geological Survey.

Hamon, W. R. (1963), Computation of direct runoff amounts from storm rainfall, *Int. Assoc. Sci. Hydrol. Publ*, *63*, 52–62, doi.

Hay, L. E., and G. J. McCabe (2002), Spatial variability in water-balance model performance in the conterminous United States, *JAWRA Journal of the American Water Resources Association*, *38*(3), 847-860, doi: 10.1111/j.1752-1688.2002.tb01001.x.

Ireson, A., C. Makropoulos, and C. Maksimovic (2006), Water Resources Modelling under Data Scarcity: Coupling MIKE BASIN and ASM Groundwater Model, *Water Resources Management*, *20*(4), 567-590, doi: 10.1007/s11269-006-3085-2.

Jefferson, A., G. Grant, and T. Rose (2006), Influence of volcanic history on groundwater patterns on the west slope of the Oregon High Cascades, *Water Resources Research*, *42*(12), W12411, doi: 10.1029/2005wr004812.

Jothityangkoon, C., M. Sivapalan, and D. L. Farmer (2001), Process controls of water balance variability in a large semi-arid catchment: downward approach to hydrological model development, *Journal of Hydrology*, *254*(1–4), 174-198, doi: 10.1016/s0022-1694(01)00496-6.

Kirkby, M. (2006), Organization and Process, in *Encyclopedia of Hydrological Sciences*, edited, John Wiley & Sons, Ltd, doi: 10.1002/0470848944.hsa003.

Klemeš, V. (1983), Conceptualization and scale in hydrology, *Journal of Hydrology*, *65*(1–3), 1-23, doi: 10.1016/0022-1694(83)90208-1.

Kokkonen, T. S., A. J. Jakeman, P. C. Young, and H. J. Koivusalo (2003), Predicting daily flows in ungauged catchments: model regionalization from catchment descriptors at the Coweeta Hydrologic Laboratory, North Carolina, *Hydrological Processes*, *17*(11), 2219-2238, doi: 10.1002/hyp.1329.

Krause, P., D. P. Boyle, and F. Bäse (2005), Comparison of different efficiency criteria for hydrological model assessment, *Adv. Geosci.*, *5*, 89-97, doi: 10.5194/adgeo-5-89-2005.

Legates, D. R., and G. J. McCabe (1999), Evaluating the use of “goodness-of-fit” Measures in hydrologic and hydroclimatic model validation, *Water Resources Research*, *35*(1), 233-241, doi: 10.1029/1998wr900018.

Li, H., M. Sivapalan, and F. Tian (2012), Comparative diagnostic analysis of runoff generation processes in Oklahoma DMIP2 basins: The Blue River and the Illinois River, *Journal of Hydrology*, *418–419*(0), 90-109, doi: http://dx.doi.org/10.1016/j.jhydrol.2010.08.005.

Li, H., M. Huang, M. S. Wigmosta, Y. Ke, A. M. Coleman, L. R. Leung, A. Wang, and D. M. Ricciuto (2011), Evaluating runoff simulations from the Community Land Model 4.0 using observations from flux towers and a mountainous watershed, *Journal of Geophysical Research: Atmospheres*, *116*(D24), D24120, doi: 10.1029/2011jd016276.

MacDonald, M. K., J. W. Pomeroy, and A. Pietroniro (2010), On the importance of sublimation to an alpine snow mass balance in the Canadian Rocky Mountains, *Hydrology and Earth System Sciences*, *14*(7), 1401-1415, doi: 10.5194/hess-14-1401-2010.

Manga, M. (1997), A model for discharge in spring-dominated streams and implications for the transmissivity and recharge of quaternary volcanics in the Oregon Cascades, *Water Resources Research*, *33*(8), 1813-1822, doi: 10.1029/97wr01339.

Martinez, G. F., and H. V. Gupta (2010), Toward improved identification of hydrological models: A diagnostic evaluation of the "abcd" monthly water balance model for the conterminous United States, *Water Resources Research*, *46*(8), W08507, doi: 10.1029/2009wr008294.

Maurer, E. P., A. W. Wood, J. C. Adam, D. P. Lettenmaier, and B. Nijssen (2002), A Long-Term Hydrologically Based Dataset of Land Surface Fluxes and States for the Conterminous United States, *Journal of Climate*, *15*(22), 3237-3251, doi: 10.1175/1520-0442(2002)015<3237:althbd>2.0.co;2.

Maxwell, R. M., and N. L. Miller (2005), Development of a Coupled Land Surface and Groundwater Model, *Journal of Hydrometeorology*, *6*(3), 233-247, doi: 10.1175/jhm422.1.

Mayer, T. D., and S. W. Naman (2011), Streamflow Response to Climate as Influenced by Geology and Elevation, *JAWRA Journal of the American Water Resources Association*, *47*(4), 724-738, doi: 10.1111/j.1752-1688.2011.00537.x.

McDonnell, J. J., and R. Woods (2004), On the need for catchment classification, *Journal of Hydrology*, *299*(1–2), 2-3, doi: 10.1016/j.jhydrol.2004.09.003.

McDonnell, J. J., M. Sivapalan, K. Vaché, S. Dunn, G. Grant, R. Haggerty, C. Hinz, R. Hooper, J. Kirchner, M. L. Roderick, J. Selker, and M. Weiler (2007), Moving beyond heterogeneity and process complexity: A new vision for watershed hydrology, *Water Resources Research*, *43*(7), W07301, doi: 10.1029/2006wr005467.

McMillan, H., B. Jackson, M. Clark, D. Kavetski, and R. Woods (2011), Rainfall uncertainty in hydrological modelling: An evaluation of multiplicative error models, *Journal of Hydrology*, *400*(1–2), 83-94, doi: http://dx.doi.org/10.1016/j.jhydrol.2011.01.026.

Mosley, M. P. (1981), Delimitation of New Zealand hydrologic regions, *Journal of Hydrology*, *49*(1-2), 173-192, doi: 10.1016/0022-1694(81)90211-0.

Nash, J. E., and J. V. Sutcliffe (1970), River flow forecasting through conceptual models part I — A discussion of principles, *Journal of Hydrology*, *10*(3), 282-290, doi: 10.1016/0022-1694(70)90255-6.

Nolin, A. W., and C. Daly (2006), Mapping "At Risk" Snow in the Pacific Northwest, *Journal of Hydrometeorology*, *7*(5), 1164-1171, doi: 10.1175/jhm543.1.

O'Connor, J. E., and G. E. Grant (2003), *A Peculiar River: Geology, Geomorphology, and Hydrology of the Deschutes River, Oregon*, 219 pp., AGU, Washington, DC.

Ogunkoya, O. O. (1988), Towards a delimitation of southwestern Nigeria into hydrological regions, *Journal of Hydrology*, *99*(1-2), 165-177, doi: 10.1016/0022-1694(88)90085-6.

Oudin, L., A. Kay, V. Andréassian, and C. Perrin (2010), Are seemingly physically similar catchments truly hydrologically similar?, *Water Resources Research*, *46*(11), W11558, doi: 10.1029/2009wr008887.

Oudin, L., V. Andréassian, T. Mathevet, C. Perrin, and C. Michel (2006), Dynamic averaging of rainfall-runoff model simulations from complementary model parameterizations, *Water Resources Research*, *42*(7), W07410, doi: 10.1029/2005wr004636.

Parajka, J., R. Merz, and G. Blöschl (2005), A comparison of regionalisation methods for catchment model parameters, *Hydrology and Earth System Sciences*, *9*(3), 157-171, doi: 10.5194/hess-9-157-2005.

Patil, S., and M. Stieglitz (2012), Modelling daily streamflow at ungauged catchments: what information is necessary?, *Hydrological Processes*, doi: 10.1002/hyp.9660.

Perrin, C., C. Michel, and V. Andréassian (2003), Improvement of a parsimonious model for streamflow simulation, *Journal of Hydrology*, *279*(1-4), 275-289, doi: 10.1016/s0022-1694(03)00225-7.

Safeeq, M., G. E. Grant, S. L. Lewis, and C. L. Tague (2013), Coupling snowpack and groundwater dynamics to interpret historical streamflow trends in the western United States, *Hydrological Processes*, *27*(5), 655-668, doi: 10.1002/hyp.9628.

Sivapalan, M., G. Blöschl, L. Zhang, and R. Vertessy (2003), Downward approach to hydrological prediction, *Hydrological Processes*, *17*(11), 2101-2111, doi: 10.1002/hyp.1425.

Slack, J. R., A. Lumb, and J. M. Landwehr (1993), Hydro-Climatic Data Network (HCDN) Streamflow Data Set, 1874-1988: *USGS Water-Resources Investigations Report 93-4076*, U.S. Geological Survey, Reston, VA.

Sophocleous, M., and S. P. Perkins (2000), Methodology and application of combined watershed and ground-water models in Kansas, *Journal of Hydrology*, *236*(3–4), 185-201, doi: 10.1016/s0022-1694(00)00293-6.

Stieglitz, M., A. Ducharne, R. Koster, and M. Suarez (2001), The Impact of Detailed Snow Physics on the Simulation of Snow Cover and Subsurface Thermodynamics at Continental Scales, *Journal of Hydrometeorology*, *2*(3), 228-242, doi: 10.1175/1525-7541(2001)002<0228:tiodsp>2.0.co;2.

Tague, C., and G. E. Grant (2004), A geological framework for interpreting the low-flow regimes of Cascade streams, Willamette River Basin, Oregon, *Water Resources Research*, *40*(4), W04303, doi: 10.1029/2003wr002629.

Tague, C., G. Grant, M. Farrell, J. Choate, and A. Jefferson (2008), Deep groundwater mediates streamflow response to climate warming in the Oregon Cascades, *Climatic Change*, *86*(1), 189-210, doi: 10.1007/s10584-007-9294-8.

Tekleab, S., S. Uhlenbrook, Y. Mohamed, H. H. G. Savenije, M. Temesgen, and J. Wenninger (2011), Water balance modeling of Upper Blue Nile catchments using a top-down approach, *Hydrology and Earth System Sciences*, *15*(7), 2179-2193, doi: 10.5194/hess-15-2179-2011.

Vaché, K. B., and J. J. McDonnell (2006), A process-based rejectionist framework for evaluating catchment runoff model structure, *Water Resources Research*, *42*(2), W02409, doi: 10.1029/2005wr004247.

Vaze, J., D. A. Post, F. H. S. Chiew, J. M. Perraud, J. Teng, and N. R. Viney (2011), Conceptual Rainfall–Runoff Model Performance with Different Spatial Rainfall Inputs, *Journal of Hydrometeorology*, *12*(5), 1100-1112, doi: 10.1175/2011jhm1340.1.

Wagener, T., M. Sivapalan, P. Troch, and R. Woods (2007), Catchment Classification and Hydrologic Similarity, *Geography Compass*, *1*(4), 901-931, doi: 10.1111/j.1749-8198.2007.00039.x.

Wigington, P. J., S. G. Leibowitz, R. L. Comeleo, and J. L. Ebersole (2012), Oregon Hydrologic Landscapes: A Classification Framework, *JAWRA Journal of the American Water Resources Association*, *49*(1), 163-182, doi: 10.1111/jawr.12009.

Wiltshire, S. E. (1986), Identification of homogeneous regions for flood frequency analysis, *Journal of Hydrology*, *84*(3-4), 287-302, doi: 10.1016/0022-1694(86)90128-9.

Winter, T. C. (2001), The Concept of Hydrologic Landscapes, *JAWRA Journal of the American Water Resources Association*, *37*(2), 335-349, doi: 10.1111/j.1752-1688.2001.tb00973.x.

Wolock, D. M., T. C. Winter, and G. McMahon (2004), Delineation and Evaluation of Hydrologic-Landscape Regions in the United States Using Geographic Information System Tools and Multivariate Statistical Analyses, *Environmental Management*, *34*(0), S71-S88, doi: 10.1007/s00267-003-5077-9.

Woods, R. (2002), Seeing catchments with new eyes, *Hydrological Processes*, *16*(5), 1111-1113, doi: 10.1002/hyp.539.

Ye, W., B. C. Bates, N. R. Viney, M. Sivapalan, and A. J. Jakeman (1997), Performance of conceptual rainfall-runoff models in low-yielding ephemeral catchments, *Water Resources Research*, *33*(1), 153-166, doi: 10.1029/96wr02840.

Young, A. R. (2006), Stream flow simulation within UK ungauged catchments using a daily rainfall-runoff model, *Journal of Hydrology*, *320*(1-2), 155-172, doi: 10.1016/j.jhydrol.2005.07.017.

Tables

Table 1: Parameter ranges for calibration of EXP-HYDRO model.

Parameter	Description	Units	Lower Limit	Upper Limit
f	Rate of decline in subsurface runoff	1/mm	0.0	0.1
S_{max}	Maximum storage of the catchment bucket	mm	100.0	1500.0
Q_{max}	Maximum subsurface runoff at full bucket	mm/day	10.0	50.0
D_f	Degree-day factor, i.e., rate of snowmelt	mm/day/°C	0.0	5.0
T_{max}	Temperature above which snow starts melting	°C	0.0	4.0
T_{min}	Temperature below which precipitation is snow	°C	-3.0	0.0

Table 2: OHL classification codes for the five physio-climatic categories (*Wigington et al.* [2012]).

Category	Classification code
Annual Climate	**V** = very wet, **W** = wet, **M** = moist, **D** = dry, **S** = semi-arid, **A** = arid
Seasonality of water surplus	**w** = winter, **s** = spring, **u** = summer
Aquifer permeability	**L** = low, **M** = medium, **H** = high
Terrain	**F** = flat, **T** = transitional, **M** = mountainous
Soil permeability	**L** = low, **M** = medium, **H** = high

Table 3: Distribution of OHL classes among the three predictability groups. Horizontal values add up to 100%. Number of catchments in Group 1 = 49, Group 2 = 14, and Group 3 = 25.

Category	% presence of OHL class					
Climate	**V**	**W**	**M**	**D**	**S**	**A**
Group 1 (0.75 < NS)	63	33	2	2	-	-
Group 2 (0.6 < NS < 0.75)	57	21	14	7	-	-
Group 3 (NS < 0.6)	24	48	16	12	-	-
Seasonality of water surplus	**w**	**s**	**u**			
Group 1 (0.75 < NS)	92	8	-			
Group 2 (0.6 < NS < 0.75)	50	50	-			
Group 3 (NS < 0.6)	28	68	4			
Aquifer permeability	**L**	**M**	**H**			
Group 1 (0.75 < NS)	84	4	12			
Group 2 (0.6 < NS < 0.75)	29	21	50			
Group 3 (NS < 0.6)	28	16	56			
Terrain	**F**	**T**	**M**			
Group 1 (0.75 < NS)	-	-	100			
Group 2 (0.6 < NS < 0.75)	-	-	100			
Group 3 (NS < 0.6)	-	-	100			
Soil permeability	**L**	**M**	**H**			
Group 1 (0.75 < NS)	39	61	-			
Group 2 (0.6 < NS < 0.75)	21	79	-			
Group 3 (NS < 0.6)	12	48	40			

Table 4: Range of the calibrated parameter values of EXP-HYDRO model among catchments belonging to each of the four OHL classes shown in Table 5. Numbers shown in parentheses are the coefficient of variation of each parameter within a given OHL class.

OHL Class	f (1/mm)	S_{max} (mm)	Q_{max} (mm/day)	D_f (mm/day/°C)	T_{min} (°C)	T_{max} (°C)
VwLML	0.011 to 0.018 (0.15)	456 to 847 (0.22)	101 to 990 (0.61)	1.08 to 4.98 (0.31)	-2.97 to -0.33 (0.50)	0.01 to 3.17 (1.01)
VwLMM	0.016 to 0.031 (0.21)	220 to 780 (0.38)	105 to 932 (0.81)	0.04 to 4.73 (0.60)	-2.95 to -0.76 (0.48)	0.66 to 3.99 (0.57)
WwLML	0.017 to 0.031 (0.25)	346 to 596 (0.20)	108 to 774 (0.76)	0.37 to 4.54 (0.81)	-1.32 to -0.34 (0.42)	1.25 to 3.84 (0.29)
WwLMM	0.012 to 0.030 (0.28)	317 to 1497 (0.58)	103 to 989 (0.77)	0.00 to 3.16 (1.84)	-2.07 to -0.01 (0.60)	1.14 to 3.98 (0.32)

Table 5: Comparison of model performance in 36 catchments when using calibrated vs. OHL class-specific average parameters. Bold values indicates catchments with > 10% model performance decline.

OHL Class	USGS Station no.	NS (calibration)	NS (average parameters)	% decline in NS
	14189500	0.925	0.922	0.33
	14193000	0.922	0.907	1.67
	14194300	0.888	0.860	3.14
	14197000	0.917	0.910	0.77
VwLML	14301500	0.898	0.887	1.20
	14303200	0.833	0.821	1.41
	14303600	0.935	0.934	0.10
	14305500	0.947	0.946	0.06
	14306100	0.873	0.871	0.24
	14141500	**0.795**	**0.709**	**10.87**
	14150300	0.853	0.851	0.18
	14161100	0.788	0.727	7.79
	14182500	0.804	0.768	4.44
	14185000	0.832	0.797	4.17
	14185900	0.780	0.744	4.64
VwLMM	14187000	0.863	0.855	0.98
	14198500	0.829	0.784	5.48
	14306340	0.857	0.849	0.90
	14306400	0.909	0.884	2.75
	14324500	0.882	0.857	2.84
	14325000	0.841	0.819	2.59
	14152500	0.798	0.784	1.82
	14156500	0.799	0.783	2.01
WwLML	**14166500**	**0.899**	**0.785**	**12.66**
	14337800	0.825	0.794	3.79
	14337870	0.687	0.633	7.88
	14338000	0.834	0.806	3.41
	14144900	**0.598**	**0.216**	**63.94**
	14150800	0.811	0.792	2.31
	14307700	0.755	0.700	7.26
	14308000	0.839	0.808	3.73
WwLMM	**14308990**	**0.569**	**0.498**	**12.54**
	14309500	0.790	0.767	2.86
	14316700	0.848	0.804	5.17
	14318000	0.766	0.722	5.70
	14371500	**0.845**	**0.722**	**14.52**

Figures

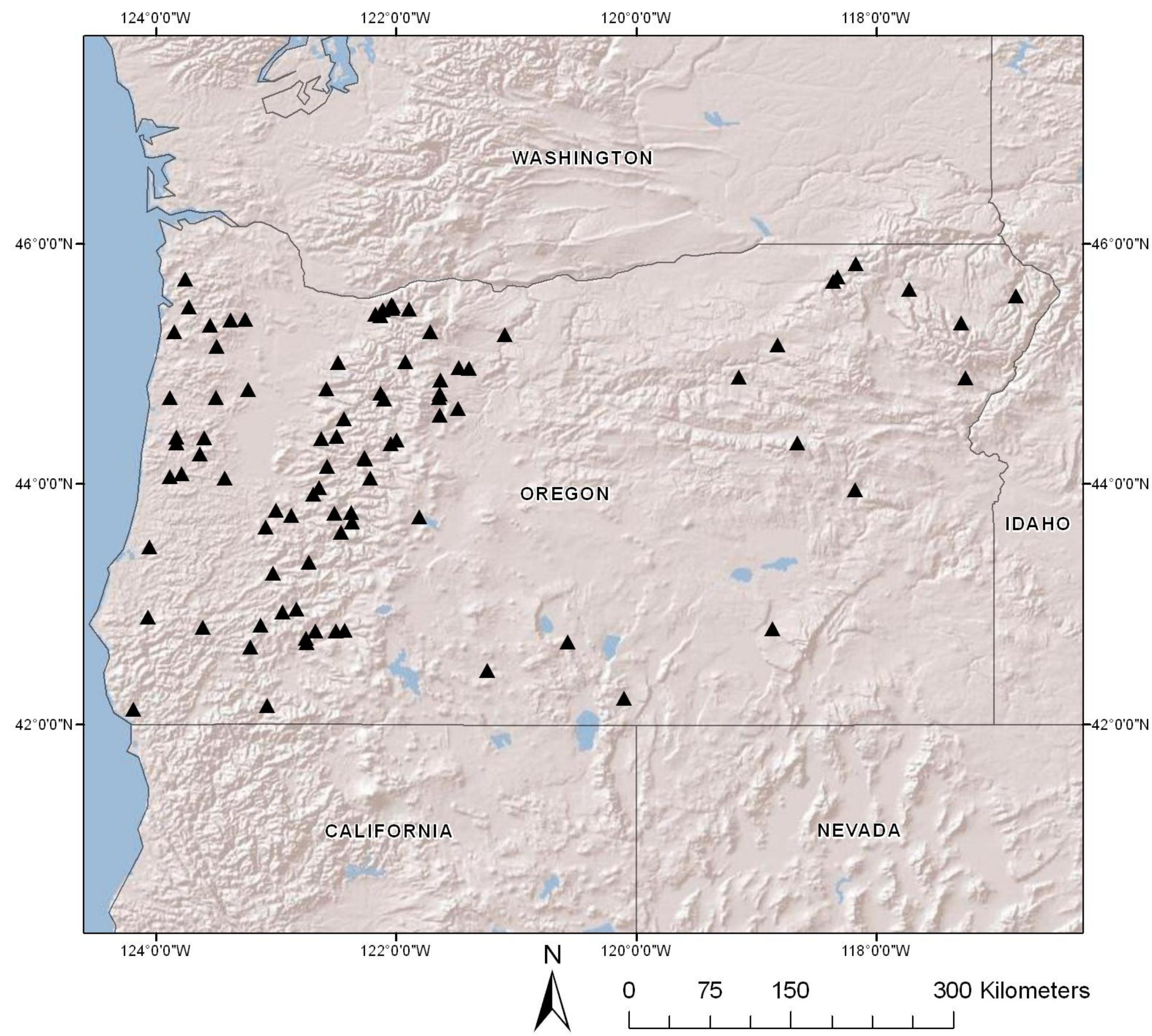

Figure 1: Location of the 88 catchment outlets within Oregon. Black triangles are the locations of catchment outlets. Map projected in WGS 1984 co-ordinate system.

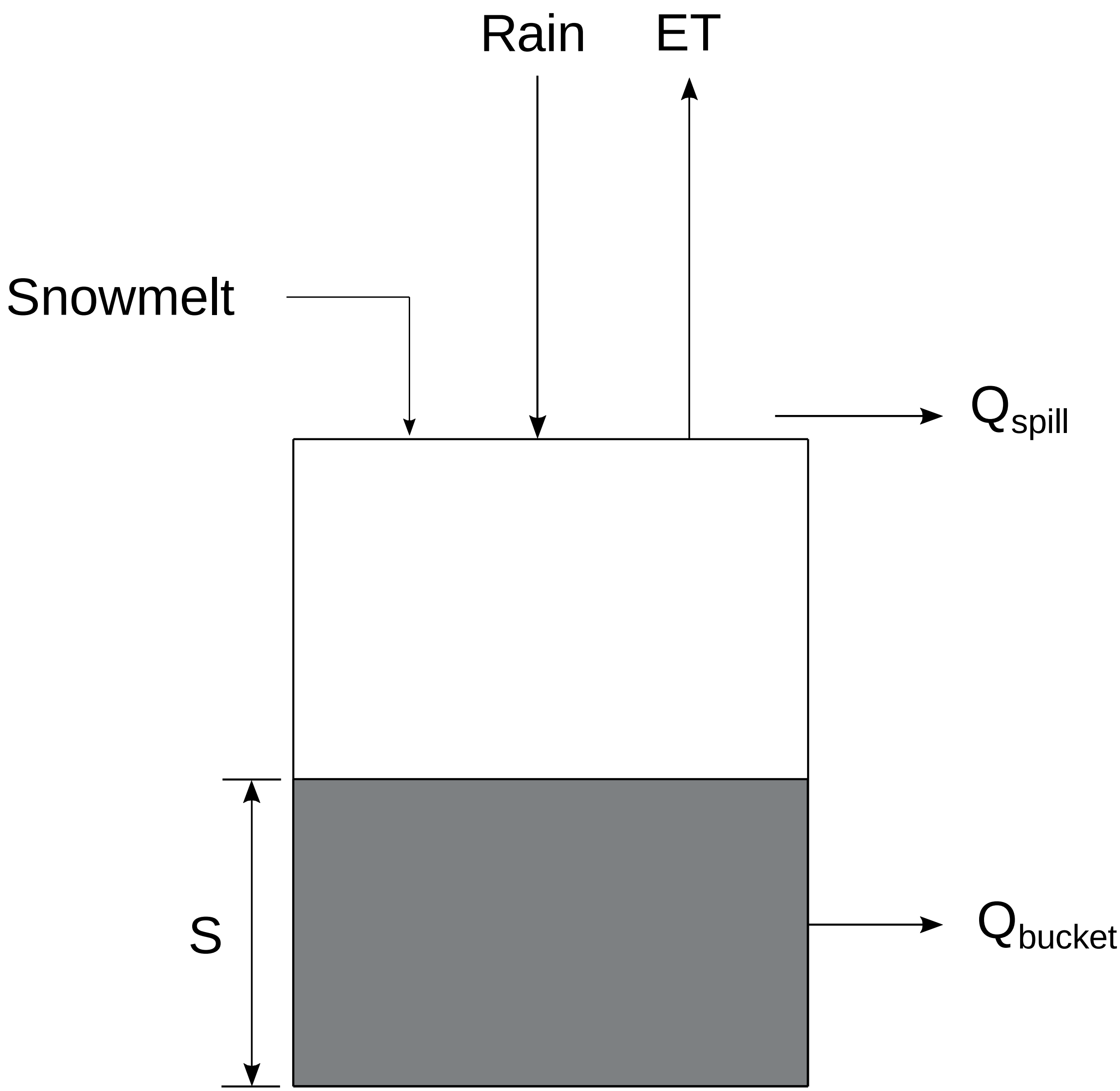

Figure 2: Schematic representation of the EXP-HYDRO model (adapted from *Patil and Stieglitz* [2012]).

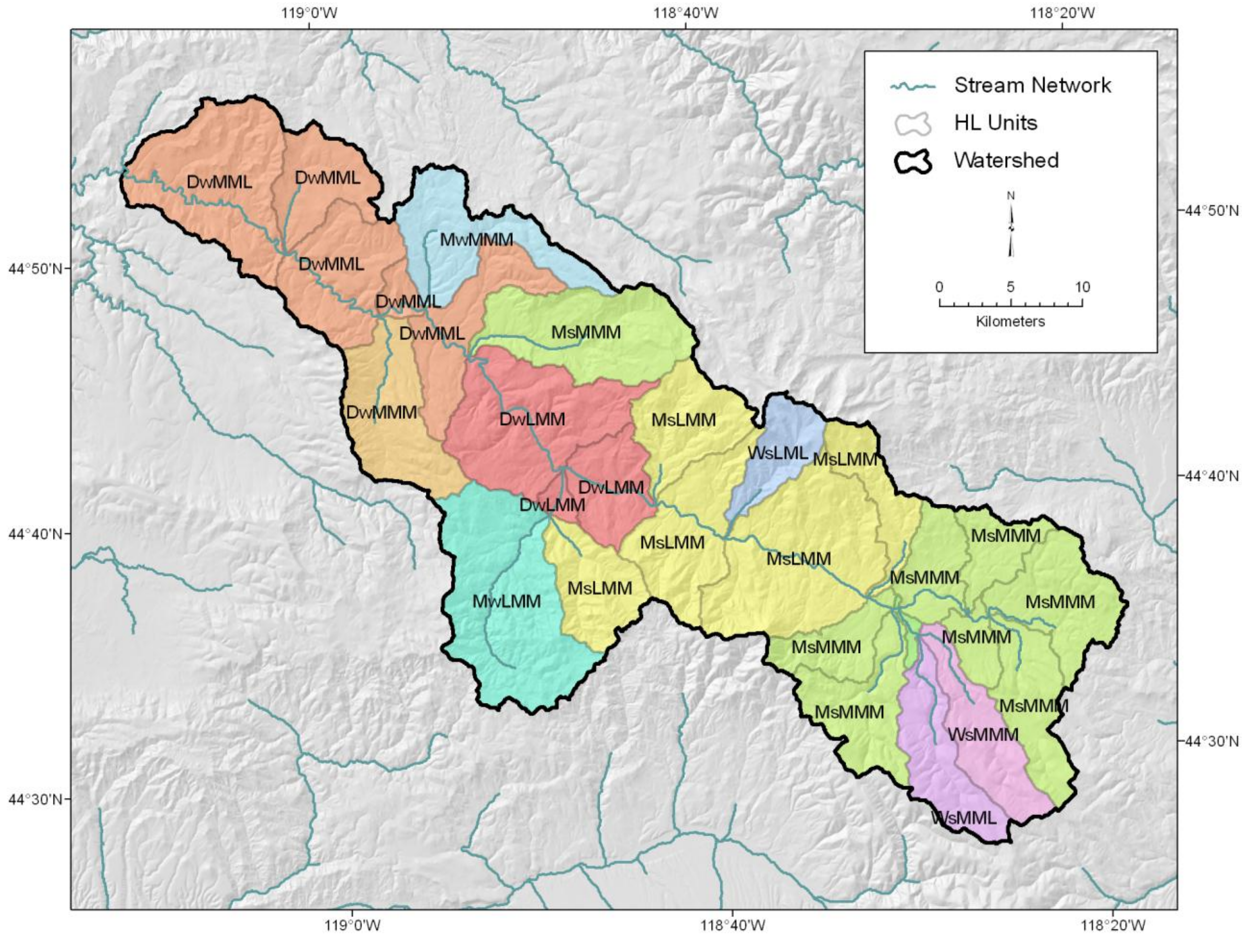

Figure 3: Map of the Middle Fork John Day River catchment showing internal heterogeneity of OHL classes at the HLU scale (Adapted from *Wigington et al.* [2012]). Map projected in UTM Zone 10 co-ordinate system.

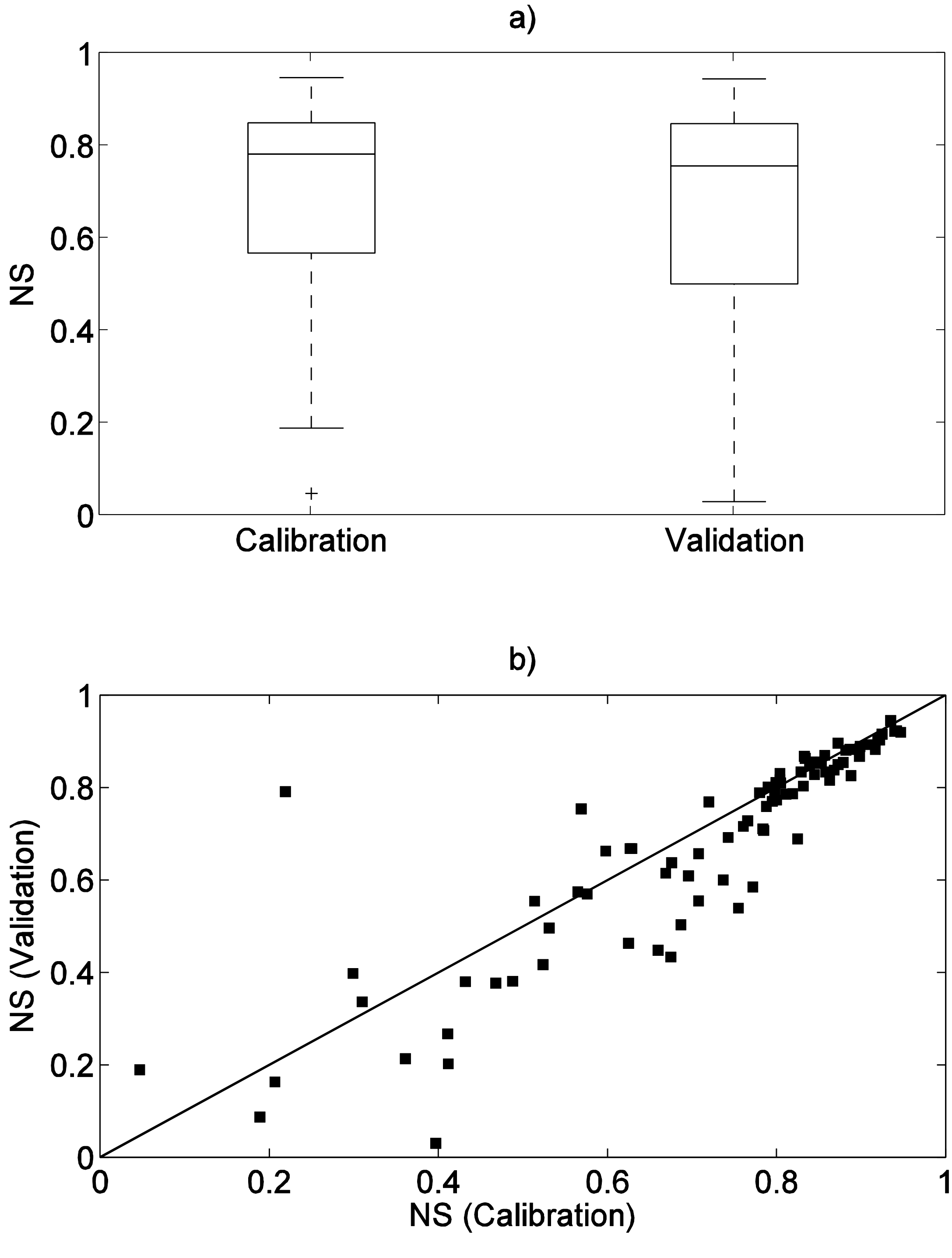

Figure 4: a) Box-and-whisker plot of NS values for calibration and validation periods, and b) 1:1 relationship of NS values for calibration and validation periods.

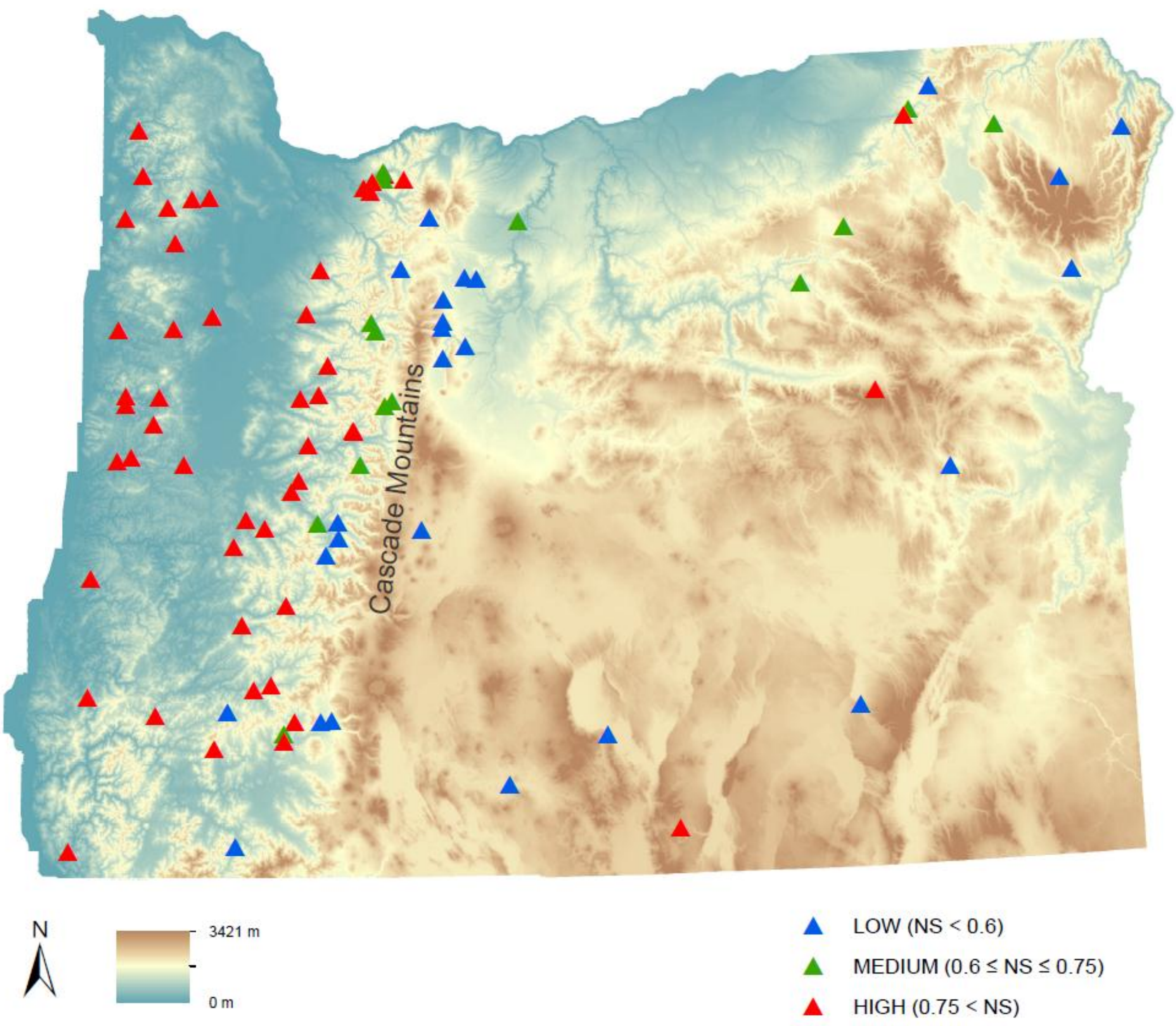

Figure 5: Classification of the 88 catchments based on calibrated NS values. Map projected in UTM Zone 10 co-ordinate system.

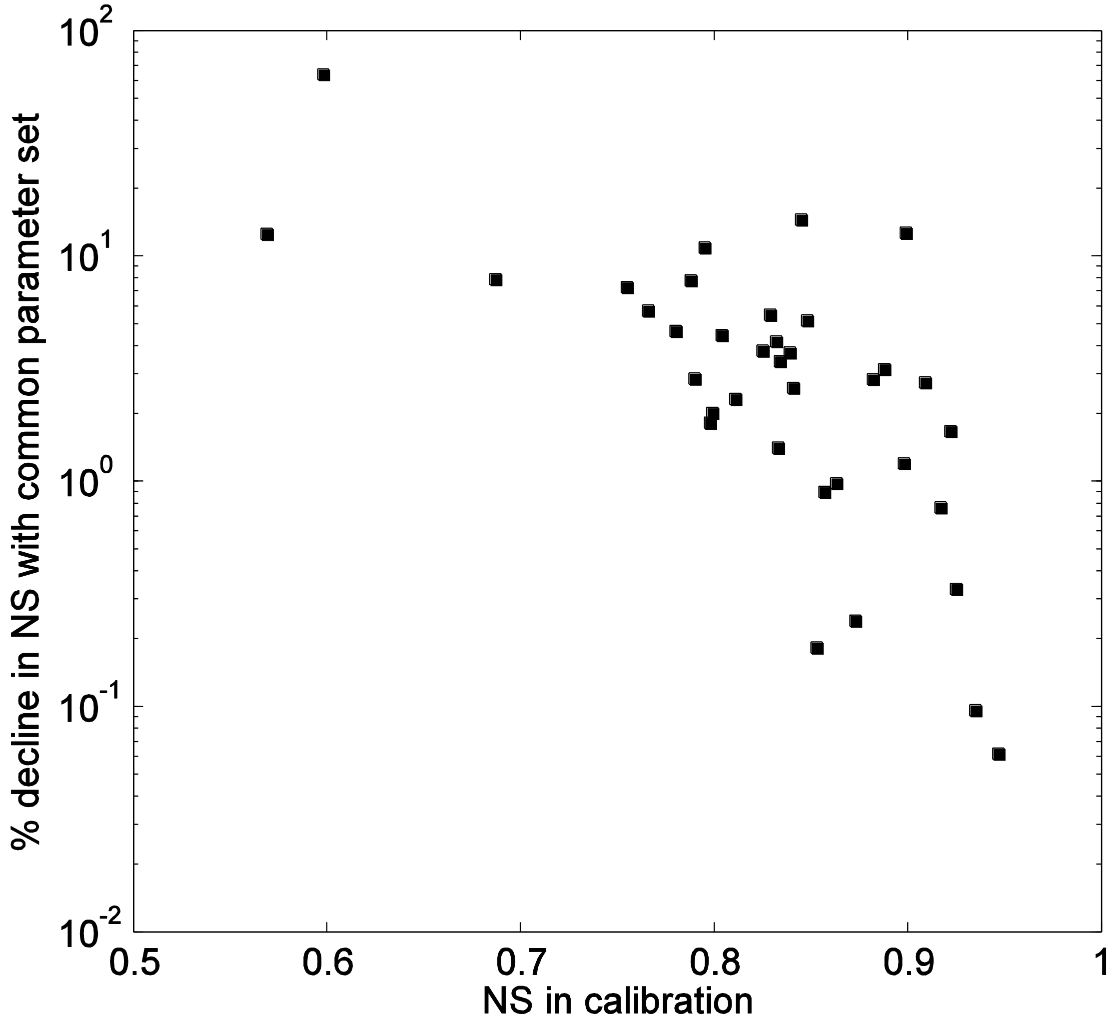

Figure 6: Relationship between calibrated NS value and the % decline in NS with class-assigned average parameter set for the subset of 36 catchments.

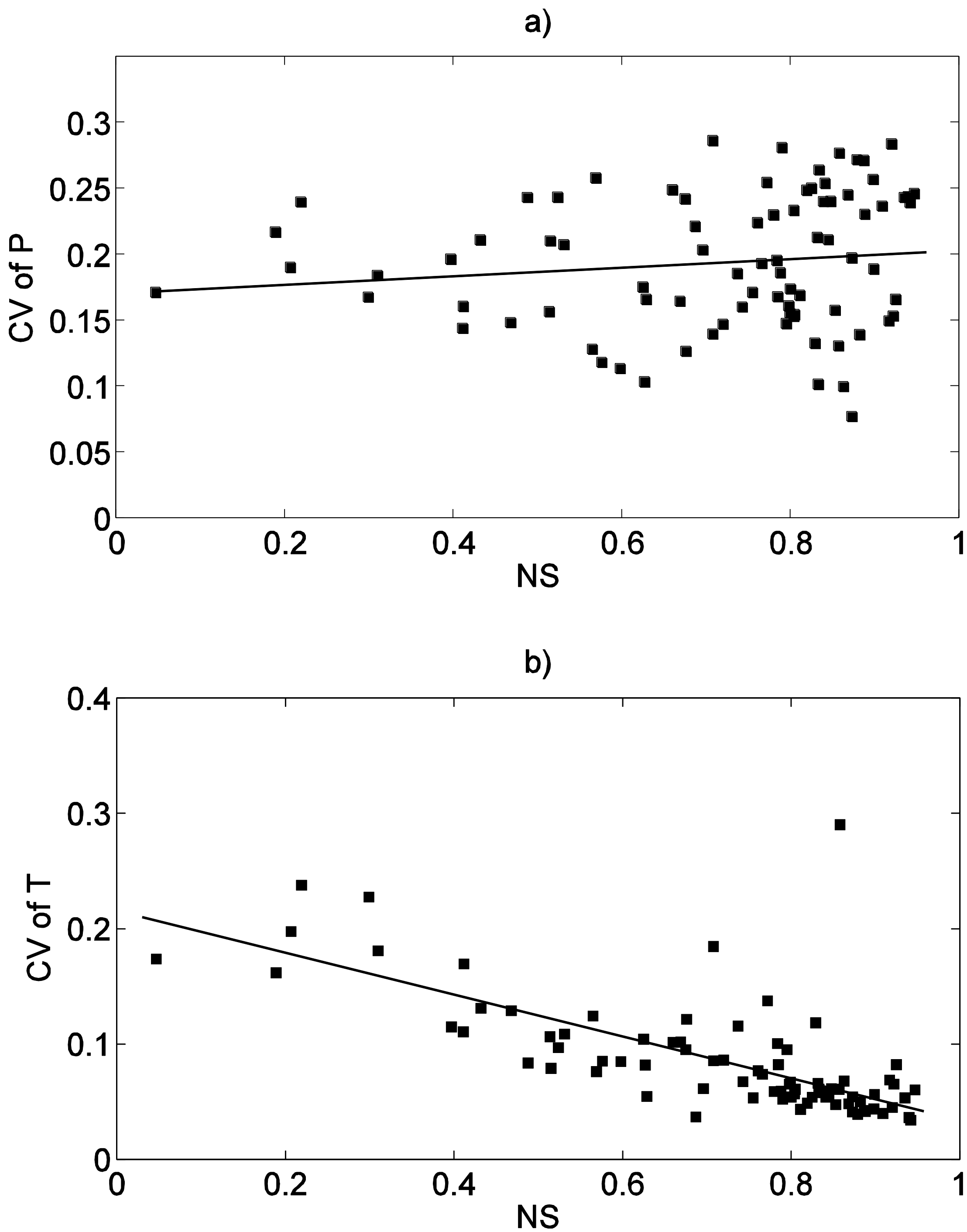

Figure 7: Relationship of calibration NS values with inter-annual coefficient of variation of a) Precipitation and b) Air temperature.

Supplementary Table S1: OHL class obtained for all 88 Oregon catchments. Numbers shown in parentheses are the percentage areal coverage of each dominant property within the catchment (indicative of spatial homogeneity).

USGS Station no.	Station Name	Climate	Seasonality of water surplus	Aquifer permeability	Terrain	Soil permeability
10370000	Camas Creek near Lakeview, OR	D (65.8)	w (65.8)	H (51.5)	M (100)	M (82.7)
10384000	Chewaucan River near Paisley, OR	M (62.5)	w (58.2)	L (58)	M (99.3)	M (73.5)
10396000	Donner and Blitzen River near Frenchglen, OR	W (41.7)	s (61.5)	M (100)	M (83.7)	M (58.3)
11497500	Sprague River near Beatty, OR	D (51.3)	w (66.8)	H (100)	M (88.4)	M (45.5)
13216500	N Fk Malheur R abv Beulah Res nr Beulah, OR	M (48.1)	s (78.5)	M (84.9)	M (100)	M (78.3)
13288200	Eagle Creek abv Skull Creek, nr New Bridge, OR	W (56.3)	s (98.8)	L (74.3)	M (100)	L (56.3)
13292000	Imnaha River at Imnaha, OR	D (41.9)	s (46.9)	M (92.1)	M (100)	L (53.3)
13329500	Hurricane Creek near Joseph, OR	W (100)	u (100)	L (100)	M (100)	L (100)
13331500	Minam River near Minam, OR	W (48.8)	s (87)	L (53)	M (100)	L (57.3)
14010000	South Fork Walla Walla River near Milton, OR	W (100)	s (100)	M (100)	M (100)	M (100)
14020000	Umatilla River abv Meacham Cr, nr Gibbon, OR	W (98.4)	s (98.4)	M (100)	M (100)	M (100)
14020300	Meacham Creek at Gibbon, OR	W (86.6)	s (80)	M (100)	M (100)	M (100)
14037500	Strawberry Cr abv Slide Cr nr Prairie City, OR	M (100)	s (100)	M (100)	M (100)	L (100)
14042500	Camas Creek near Ukiah, OR	M (100)	s (97.3)	M (100)	M (97.7)	M (100)
14044000	Middle Fork John Day River at Ritter, OR	M (57.8)	s (59.2)	M (85)	M (76.4)	M (83.8)
14054500	Brown Creek near La Pine, OR	W (100)	s (100)	H (100)	M (100)	H (100)
14090350	Jefferson Creek near Camp Sherman, OR	V (100)	s (100)	H (100)	M (100)	H (100)

14090400	Whitewater River near Camp Sherman, OR	W (100)	s (100)	H (100)	M (100)	H (100)
14091500	Metolius River near Grandview, OR	W (53.8)	s (62.7)	H (100)	M (99.8)	H (100)
14092750	Shitike Cr, at Peters Pasture, nr Warm Springs, OR	M (100)	w (100)	H (100)	M (100)	H (100)
14095500	Warm Springs River near Simnasho, OR	W (79.5)	s (79.5)	H (100)	M (96.7)	H (82.9)
14096300	Mill Creek, nr Badger Butte, nr Warm Springs, OR	W (100)	s (100)	H (100)	M (100)	H (100)
14096850	Beaver Creek, blw Quartz Cr, nr Simnasho, OR	D (57.4)	w (100)	L (50.6)	M (92.6)	H (72.7)
14101500	White River below Tygh Valley, OR	D (38.1)	w (67)	H (93.4)	M (87.8)	L (47.9)
14134000	Salmon River near Government Camp, OR	V (100)	s (100)	H (100)	M (100)	M (100)
14137000	Sandy River near Marmot, OR	V (100)	s (74.6)	H (73.8)	M (100)	M (90.7)
14138800	Blazed Alder Creek near Rhododendron, OR	V (100)	s (100)	H (100)	M (100)	M (100)
14138870	Fir Creek near Brightwood, OR	V (100)	w (100)	H (100)	M (100)	M (100)
14138900	North Fork Bull Run River near Multnomah Falls, OR	V (100)	w (100)	H (100)	M (100)	M (100)
14139700	Cedar Creek near Brightwood, OR	V (100)	w (100)	H (100)	M (100)	M (100)
14139800	South Fork Bull Run River near Bull Run, OR	V (100)	w (100)	H (100)	M (100)	M (100)
14141500	Little Sandy River near Bull Run, OR	V (100)	w (100)	L (100)	M (100)	M (100)
14144800	Middle Fork Willamette River nr Oakridge, OR	V (55.8)	s (55.8)	H (68)	M (100)	M (63.7)
14144900	Hills Cr abv Hills Cr Res, nr Oakridge, OR	W (100)	w (100)	L (100)	M (100)	M (100)
14146500	Salmon Creek near Oakridge, OR	V (64.7)	s (64.7)	H (75.1)	M (56.3)	M (56.3)
14147500	N Fk of M Fk Willamette R nr Oakridge, OR	V (51.3)	w (73.9)	H (53.9)	M (100)	M (59.4)

14150300	Fall Creek near Lowell, OR	V (60.5)	w (100)	L (100)	M (100)	M (71.1)
14150800	Winberry Creek near Lowell, OR	W (100)	w (100)	L (100)	M (100)	M (80.2)
14152500	Coast Fork Willamette River at London, OR	W (100)	w (100)	L (100)	M (100)	L (100)
14154500	Row River near Dorena, OR	W (78.7)	w (100)	L (100)	M (100)	M (72.4)
14156500	Mosby Cr at mouth, nr Cottage Grove, OR	W (100)	w (100)	L (100)	M (100)	L (100)
14158500	McKenzie River at outlet of Clear Lake, OR	V (100)	s (100)	H (100)	M (99)	M (76.1)
14158790	Smith R abv Smith R res nr Belknap Springs, OR	V (100)	s (100)	H (100)	M (100)	M (100)
14159200	So Fk McKenzie River abv Cougar Lk nr Rainbow, OR	V (100)	w (60.5)	L (56.3)	M (100)	M (100)
14161100	Blue River below Tidbits Creek, nr Blue River, OR	V (100)	w (100)	L (100)	M (100)	M (100)
14161500	Lookout Creek near Blue River, OR	V (100)	w (100)	H (100)	M (100)	M (100)
14163000	Gate Creek at Vida, OR	V (61.4)	w (100)	L (100)	M (100)	L (52)
14166500	Long Tom River near Noti, OR	W (100)	w (100)	L (99.1)	M (98.8)	L (100)
14178000	North Santiam River below Boulder Cr, nr Detroit, OR	V (100)	s (80.4)	H (94.2)	M (100)	M (54.3)
14179000	Breitenbush R abv French Cr nr Detroit, OR	V (100)	w (56.6)	L (56.6)	M (100)	M (56.6)
14182500	Little North Santiam River near Mehama, OR	V (100)	w (100)	L (100)	M (100)	M (100)
14185000	South Santiam below Cascadia, OR	V (91.9)	w (100)	L (100)	M (100)	M (81.5)
14185900	Quartzville Creek near Cascadia, OR	V (100)	w (100)	L (100)	M (100)	M (100)
14187000	Wiley Creek near Foster, OR	V (98.8)	w (100)	L (100)	M (100)	M (66.3)
14189500	Luckiamute River near Hoskins, OR	V (100)	w (100)	L (100)	M (100)	L (100)

14190500	Luckiamute River near Suver, OR	W (53.1)	w (100)	L (96.1)	M (70)	L (53.1)
14193000	Willamina Creek near Willamina, OR	V (96.1)	w (100)	L (100)	M (96.1)	L (100)
14194300	North Yamhill River near Fairdale, OR	V (100)	w (100)	L (100)	M (100)	L (100)
14197000	North Yamhill R at Pike, OR	V (64.8)	w (100)	L (100)	M (100)	L (100)
14198500	Molalla R abv PC nr Wilhoit, OR	V (100)	w (100)	L (100)	M (100)	M (100)
14208000	Clackamas River at Big Bottom, OR	V (100)	s (88.3)	H (100)	M (99.7)	M (73.2)
14301000	Nehalem River near Foss, OR	V (75.9)	w (100)	L (98)	M (85.5)	L (55.9)
14301500	Wilson River near Tillamook, OR	V (100)	w (100)	L (100)	M (100)	L (100)
14303200	Tucca Creek near Blaine, OR	V (100)	w (100)	L (100)	M (100)	L (100)
14303600	Nestucca River near Beaver, OR	V (100)	w (100)	L (100)	M (100)	L (94)
14305500	Siletz River at Siletz, OR	V (100)	w (100)	L (100)	M (98.1)	L (63.3)
14306100	N Fk Alsea R at Alsea, OR	V (76.9)	w (100)	L (100)	M (100)	L (100)
14306340	East Fork Lobster Creek near Alsea, OR	V (100)	w (100)	L (100)	M (100)	M (100)
14306400	Five Rivers nr Fisher, OR	V (100)	w (100)	L (100)	M (100)	M (100)
14306500	Alsea River near Tidewater, OR	V (70)	w (100)	L (100)	M (100)	M (51.1)
14307580	Lake Creek near Deadwood, OR	V (53)	w (100)	L (100)	M (100)	M (100)
14307620	Siuslaw River near Mapleton, OR	W (64.8)	w (100)	L (100)	M (99.9)	M (59)
14307700	Jackson Creek nr Tiller, OR	W (100)	w (100)	L (100)	M (100)	M (100)
14308000	South Umpqua River at Tiller, OR	W (100)	w (100)	L (100)	M (100)	M (100)

14308990	Cow Creek abv Galesville res, nr Azalea, OR	W (100)	w (100)	L (80.6)	M (100)	M (80.6)
14309500	West Fork Cow Creek near Glendale, OR	W (100)	w (100)	L (100)	M (100)	M (100)
14316700	Steamboat Creek near Glide, OR	W (83.1)	w (100)	L (100)	M (100)	M (100)
14318000	Little River at Peel, OR	W (94)	w (100)	L (100)	M (100)	M (77.1)
14324500	West Fork Millicoma River near Allegany, OR	V (100)	w (100)	L (100)	M (100)	M (100)
14325000	South Fork Coquille River at Powers, OR	V (86.3)	w (100)	L (100)	M (100)	M (99.3)
14328000	Rogue River above Prospect, OR	V (68.3)	s (71)	H (69.2)	M (99.4)	H (78.9)
14333500	Red Blanket Creek near Prospect, OR	W (100)	s (100)	H (100)	M (100)	H (100)
14337800	Elk Creek near Cascade Gorge, OR	W (100)	w (100)	L (100)	M (99.7)	L (100)
14337870	West Branch Elk Creek near Trail, OR	W (100)	w (100)	L (100)	M (100)	L (100)
14338000	Elk Creek near Trail, OR	W (97.1)	w (100)	L (100)	M (99.8)	L (100)
14362250	Star Gulch near Ruch, OR	M (100)	w (100)	L (100)	M (100)	M (100)
14371500	Grave Creek at Pease Bridge, near Placer, OR	W (100)	w (100)	L (100)	M (100)	M (100)
14400000	Chetco River near Brookings, OR	V (100)	w (100)	L (81.1)	M (100)	L (55.8)